JACS
JOURNAL OF THE AMERICAN CHEMICAL SOCIETY

Article

pubs.acs.org/JACS

Photoinduced Bending of Self-Assembled Azobenzene–Siloxane Hybrid

Sufang Guo,[†] Kimihiro Matsukawa,[‡] Takashi Miyata,[§] Tatsuya Okubo,[∥] Kazuyuki Kuroda,[#,¶] and Atsushi Shimojima*[,#]

[†]Institute for Nanoscience & Technology, Waseda University, 513 Wasedatsurumaki-cho, Shinjuku-ku, Tokyo 162-0041, Japan

[‡]Electronic Materials Research Division, Osaka Municipal Technical Research Institute, 1-6-50 Morinomiya, Joto-ku, Osaka 536-8553, Japan

[§]Department of Chemistry and Materials Engineering, Kansai University, 3-3-35 Yamate-cho, Suita-shi, Osaka 564-8680, Japan

[∥]Department of Chemical System Engineering, The University of Tokyo, 7-3-1 Hongo, Bunkyo-ku, Tokyo 113-8656, Japan

[#]Department of Applied Chemistry, Waseda University, 3-4-1 Ohkubo, Shinjuku-ku, Tokyo 169-8555, Japan

[¶]Kagami Memorial Research Institute for Materials Science and Technology, Waseda University, 2-8-26 Nishiwaseda, Shinjuku-ku, Tokyo 169-0051, Japan

Supporting Information

ABSTRACT: A novel azobenzene–siloxane hybrid material displaying photoinduced macroscopic motions has been prepared by one-step organosilane self-assembly. Two types of alkoxysilane precursors with either pendant or bridging azobenzene groups were synthesized via thiol–ene click reactions. Hybrid films with well-ordered lamellar structures were obtained by hydrolysis and polycondensation of these precursors. The film with solely pendant azobenzene groups showed reversible and rapid *d*-spacing variation upon UV–vis irradiation, which was induced by the *trans*–*cis* isomerization of azobenzene moieties. The flexible, free-standing film obtained by co-condensation of two types of precursors showed reversible bending–unbending motions upon UV–vis irradiation. The partial cross-linking between the siloxane layers by bridging azobenzene groups was crucial for photoinduced distortion of the film. This film possesses high elastic modulus, good thermal stability, and shows large amplitude of photoinduced bending–unbending over a wide temperature range. This is the first report on photoinduced macroscopic motions of azobenzene-containing siloxane-based materials. These materials possess great potential for applications in smart devices and energy conversion systems.

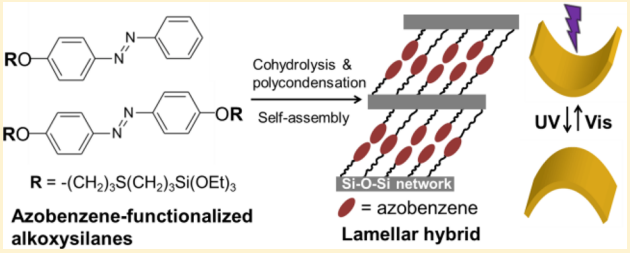

INTRODUCTION

Photoresponsive materials are attracting extensive research interest for their significance in science and applications.[1] Azobenzene is one of the most widely utilized chromophores for producing photoresponsive materials. It reversibly isomerizes between the *trans* and *cis* isomers upon UV–vis irradiation, producing dramatic changes in size and polarity.[2] Research on photoinduced deformations/motions in azobenzene-containing materials has been flourishing due to their potential applications as smart sensors, motors, actuators, etc. Finkelmann et al. first reported in-plane photocontraction in azobenzene-containing liquid crystal elastomers (LCEs).[3] Liquid crystal (LC) polymer films capable of expanding–contracting,[4] bending–unbending,[5−9] and other three-dimensional movements[10−12] upon light irradiation have been reported subsequently. Ikeda et al. achieved exciting photoresponsive motions in LC polymers where azobenzene moieties are covalently bonded to the lightly cross-linked hydrocarbon backbones.[5,10,11,13] Intrinsic flexibility of the soft materials is preferable to realize effective *trans*–*cis* photoisomerization of azobenzene. Broer et al.[9] and White et al.[8] have reported photoinduced bending of glassy LC polymer networks (LCNs) with high elastic moduli; however, these materials generally show lower deformation magnitude compared to the LCEs. By employing high intensity irradiation, relatively large, high frequency oscillations have been achieved.[14]

Extensive efforts and progress have also been made with photoresponsive inorganic–azobenzene nanocomposites, in which the inorganic moiety can impart mechanical, thermal, and chemical stability. Layered inorganic compounds intercalated with azobenzene derivatives through electrostatic interactions show photoinduced reversible *d*-spacing changes[15−17] and muscle-like sliding of nanosheets.[16] Azobenzenes grafted on the pore surface[18−21] or integrated in the framework[22,23] of mesoporous silica allow manipulation of pore size and controlled release of guest molecules upon light irradiation. However, to the best of our knowledge, photo-

Received: June 13, 2015
Published: November 17, 2015

DOI: 10.1021/jacs.5b06172
J. Am. Chem. Soc. 2015, 137, 15434−15440

induced macroscopic motions such as bending have not been reported, most likely due to the difficulty of morphology control and/or the excessive rigidity of the inorganic frameworks.

Ordered organosiloxane hybrids designed at the molecular scale[24] are promising candidates to address these issues. The organosiloxane network containing Si−C bonds is highly stable, capable of forming various structures and morphologies, and basically transparent in the UV and visible regions. A few reports exist on the synthesis of azobenzene-containing LCEs with linear polysiloxane backbones, which act as flexible and elastic matrix for photo- and heat-induced deformation and generation of stress during nematic-to-isotropic transition.[3,25] As a new class of azobenzene-functionalized organosiloxanes with more cross-linked siloxane networks, Liu et al. reported the preparation of lamellar hybrids through self-assembly of an azobenzene-bridged bis-trialkoxysilane precursor having hydrogen-bonding urea linkages.[26] Although highly ordered structures were obtained, *trans*−*cis* photoisomerization in these materials was inhibited probably due to intense hydrogen-bonding interactions. More recently, we reported that azobenzene-functionalized trialkoxysilane precursors with simple propylene spacers can self-assemble into lamellar structures.[27] Slight reversible *d*-spacing changes were observed upon partial *trans*−*cis* photoisomerization; however, photoinduced macroscopic motions in such self-assembled hybrid systems has not yet been achieved.

Herein, we report a photodeformable hybrid material prepared by self-assembly of newly designed organotrialkoxysilane precursors with pendant and bridging azobenzene groups (**P1** and **P2**, respectively, in Figure 1). The relatively

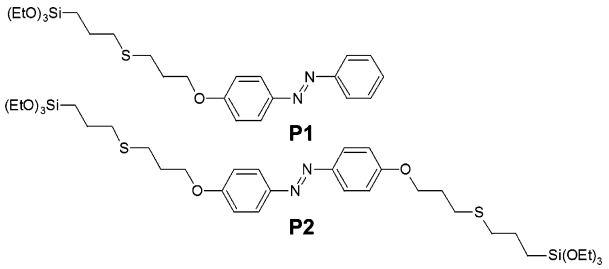

Figure 1. Organoalkoxysilane precursors with pendant and bridging azobenzene groups (**P1** and **P2**, respectively).

long organic spacers between azobenzene and Si atoms are expected to increase the hydrophobic interactions for self-assembly. Additionally, the introduction of $-CH_2-S-CH_2-$ linkages may inhibit close packing of the spacer chains, thus increasing the flexibility and free volume of the networks. In addition to photoresponsive lamellar thin films from each precursor, a free-standing film showing reversible bending−unbending motions upon UV−vis irradiation was successfully obtained from a mixture of **P1** and **P2**. The bridging azobenzene moieties derived from **P2** has contributed to the improvement of stability as well as the achievement of bending−unbending motions. This is the first to demonstrate photoinduced motions in relatively rigid organosiloxane hybrids, which are intrinsically different from conventional "soft" polymer-based materials.

RESULTS AND DISCUSSION

Spin-coating of the tetrahydrofuran (THF) solutions of hydrolyzed **P1** and **P2** on glass substrates gave yellow transparent thin films (**H1** and **H2**, respectively). Formation of siloxane networks in both films was confirmed by the significant decrease of the $SiOCH_2CH_3$ absorption band ($\nu_{as}(CH_3)$ at ca. 2971 cm^{-1}) and appearance of a strong Si−O−Si band (ν_{as}(Si−O−Si) at around 1100 cm^{-1}) in the Fourier transform infrared (FT-IR) spectra (Figure S1 in the Supporting Information (SI)). The X-ray diffraction (XRD) patterns of **H1** and **H2** (Figure 2A) show sharp diffraction

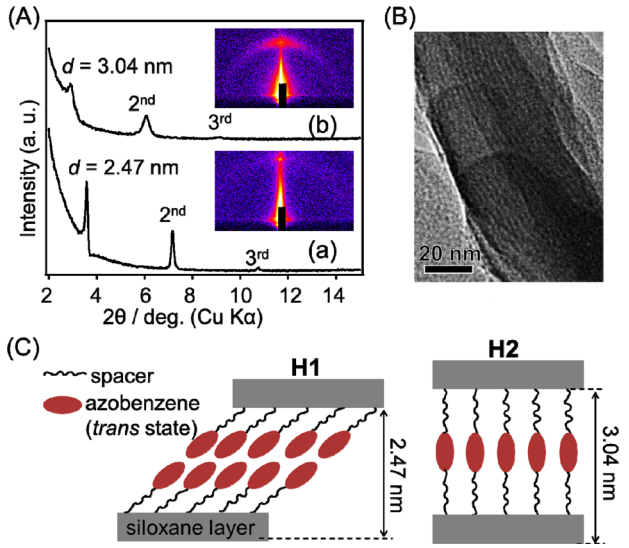

Figure 2. (A) XRD patterns of (a) **H1** and (b) **H2**; insets are their 2D-XRD images. (B) TEM image of **H2**, which was peeled off from the substrate and pulverized for observation. (C) Possible arrangements of azobenzene groups in **H1** and **H2**. The average tilt angle of azobenzene groups in **H1** was calculated to be approximately 38°, assuming a bilayer structure with fully extended organic groups.

peaks with *d*-spacings of 2.47 and 3.04 nm, respectively, along with second- and third-order peaks. The 2D-XRD images (Figure 2A, insets) show single spots on the vertical axis, indicating formation of lamellar structures oriented parallel to the substrate. The transmission electron microscopy (TEM) image of **H2** (Figure 2B) shows a striped texture with a periodicity of ca. 2.9 nm, which roughly corresponds to the *d*-spacing. TEM observation of **H1** was unsuccessful due to its instability under electron beam irradiation.

Taking into account the molecular lengths of **P1** (2.01 nm between Si and the terminal C of the azobenzene group) and **P2** (3.25 nm between two Si atoms) in fully extended states (Figure S2 in SI), the structural models of **H1** and **H2** were deduced, as shown in Figure 2C. We assumed that the azobenzene moieties in **H1** were in a tilted bilayer arrangement rather than an interdigitated monolayer arrangement, based on our previous study on alkylsiloxane mesophases that form an interdigitated monolayer only when additional SiO_4 species are introduced to increase the lateral distance between the alkylsilyl groups.[24a] It is reasonable to consider that azobenzenes in **H2** are arranged to form a monolayer oriented almost perpendicular to the substrate.

Photoisomerization of azobenzene moieties in lamellar hybrids **H1** and **H2** was investigated by UV−vis spectroscopy. Generally, the wavelength of the absorption of *trans* isomers

DOI: 10.1021/jacs.5b06172
J. Am. Chem. Soc. 2015, 137, 15434−15440

and the degree of *trans*–*cis* photoisomerization reflect the packing state and mobility of azobenzenes.[23,28] For **H1** (Figure 3a, red), the absorption peak due to the π–π^* transition of the

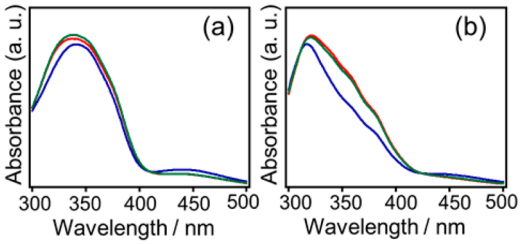

Figure 3. UV–vis spectra of (a) **H1** and (b) **H2**; before irradiation (red), after 1 min of UV irradiation (blue), and after 1 min of subsequent visible light irradiation (green) at room temperature.

trans isomer is observed at ca. 345 nm, which is similar to that for **P1** in a THF solution (Figure S3 in SI), implying a loosely packed state of the interlayer azobenzene groups. Conversely, the absorption peak at approximately 320 nm for **H2** (Figure 3(b), red) is largely blue-shifted from that of **P2** in THF (357 nm), indicating that the azobenzene groups are closely packed in the H-aggregates.[28]

When **H1** and **H2** were exposed to UV light, the peak for *trans* isomers decreased slightly and that for the n–π^* transition of the *cis* isomers (at approximately 450 nm) increased (Figure 3, blue). After subsequent visible light irradiation, both spectra returned to their original shape (Figure 3, green). This demonstrates partial but reversible photoisomerization of the azobenzene groups in these samples. The degree of isomerization was apparently smaller than that in solution state and remained almost unchanged even when the irradiation time was further increased, suggesting that steric hindrance existed in the interlayer spaces. Nonetheless, it is important to note that isomerization is not completely restricted in **H2**. This is in contrast to our previous report,[27b] in which photoisomerization of azobenzene groups was completely inhibited in the lamellar hybrid prepared from an azobenzene-bridged precursor containing propylene spacers. The longer, flexible, sulfur-containing spacers in **P2** have thus improved the mobility of azobenzenes.

The partial photoisomerization of azobenzene groups in **H1** was found to induce variations in the lamellar periodicity. After 1 min of UV irradiation on **H1**, the XRD peaks shifted to higher diffraction angles (Figure 4A(b)), indicating a decrease in the *d*-spacing (ca. 0.06 nm, corresponding to ca. 3% of the original value). After subsequent visible light irradiation for 1 min, the peaks returned to their original positions (Figure 4A(b′)). These shifts can be associated with the *trans*-to-*cis* and *cis*-to-*trans* isomerization of interlayer azobenzene groups (Figure 3A). It is generally observed that conversion from the rod-like *trans* isomer to the bent *cis* isomer induces a decrease or loss of structural order (e.g., a nematic to isotropic transition) in conventional LC polymers.[4,5,13] The high order of the lamellar structure of **H1** even after UV irradiation is attributable to the two-dimensional (2D) siloxane network, which is in clear contrast to the linear backbone of LC polymers. The degree of polycondensation is also important; when the as-synthesized film before heating (see Experimental Section) was exposed to UV light, a loss of lamellar order was observed.

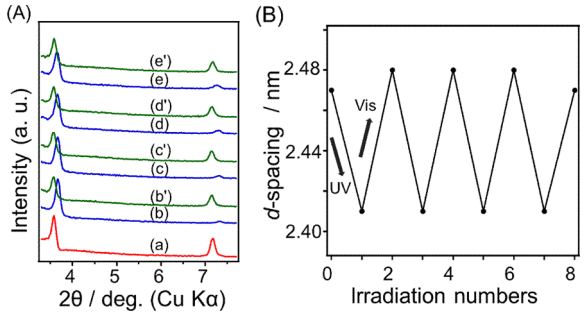

Figure 4. (A) Variation of XRD patterns of **H1**; (a) before irradiation (red), (b, b′) after 1 min, (c, c′) after 30 s, (d, d′) after 16 s, and (e, e′) after 10 s of UV irradiation (blue) and subsequent visible light irradiation (green) at room temperature. (B) *d*-Spacing variation of **H1** during the four cycles of UV–vis irradiation. The irradiations were performed in the above sequence on the same sample.

Reversible *d*-spacing variations of 0.06–0.07 nm were also observed even when the irradiation time was shortened to 30, 16, and 10 s (Figure 4A(c–e′) and 4B). In the case of the lamellar hybrid containing propylene spacers,[27a] ca. 5 min of irradiation was required to reach the maximum decrease in *d*-spacing (ca. 0.04 nm). Thus, much faster and larger *d*-spacing variations have been realized by utilizing a newly designed precursor. This is attributed to the long and flexible spacers between the azobenzene groups and the siloxane layer. However, although reversible *trans*–*cis* photoisomerization (Figure 3b) also occurred in **H2**, there was no change in the XRD pattern (Figure S4 in SI), most likely due to the higher rigidity of the completely azobenzene-bridged network.

Such a photoresponse property of **H1** can be utilized to induce macroscopic deformation. Photoinduced bending–unbending motions have been reported for azobenzene-containing LC gels, elastomers, and glassy networks;[5–9] however, similar motions in inorganic–organic hybrid systems are unprecedented. First, we tried to prepare a thick, free-standing film of **H1** by casting the hydrolyzed solution on a substrate coated with a sacrificial poly(vinyl alcohol) (PVA) layer. The resulting film was fragile and easily broken into small fragments when peeled from the substrate, and the small fragments of the film did not show obvious deformation upon UV irradiation. Unexpectedly, we found that when **P1** and **P2** were mixed (molar ratio of 4:1), a smooth and flexible free-standing film (**H3**) showing reversible bending–unbending motions was successfully obtained.

The XRD pattern of **H3** (Figure 5(a)) confirmed the formation of a single lamellar phase with *d*-spacing (2.64 nm) slightly larger than that of **H1** (2.47 nm), suggesting that the bridge-type precursor was incorporated into the bilayer

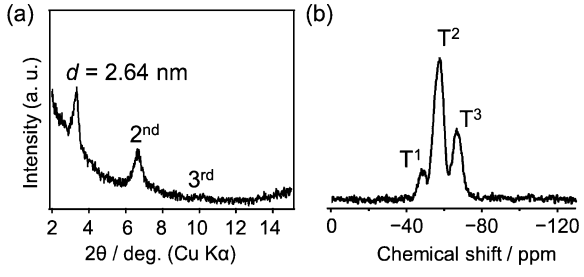

Figure 5. (a) XRD pattern and (b) ^{29}Si cross-polarization magic-angle spinning (CP/MAS) NMR spectrum of **H3**.

DOI: 10.1021/jacs.5b06172
J. Am. Chem. Soc. 2015, 137, 15434–15440

structure of **H1** without phase separation. UV−vis spectra of the thin film prepared by spin-coating (Figure S5 in SI) showed partial *trans*−*cis* isomerization upon UV−vis irradiation similar to that observed for **H1**. We confirmed that both thermal and chemical stability were improved by incorporation of bridging azobenzene groups. When heated at 100 °C or immersed in 1,4-dioxane, the lamellar structure of **H1** collapsed, while **H3** remained intact. These increased stabilities can be explained by covalent linking of the siloxane layers by bridging azobenzene groups derived from **P2**.

H3 was flexible enough to be bent by tweezers without being broken (Figure S6 in SI). The film was cut into a rectangular shape and placed on the tweezers (Figure 6A(a)) to test the

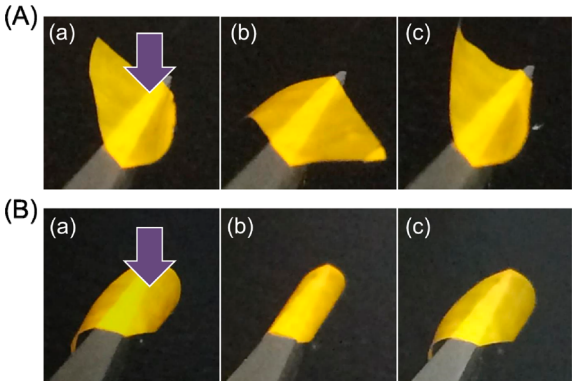

Figure 6. Bending−unbending behaviors of **H3** upon UV−vis irradiation from (A) the upper side and (B) the reverse side of the horizontally supported film at room temperature. Film size: approximately 7 mm × 3 mm × 3.2 μm. The purple arrows indicate the direction of irradiation.

photoinduced motions. Upon UV irradiation, bending of the film away from the UV source was observed. The initially curved film first became flat and then gradually curved downward within 1 min (Figure 6A(b) and Movie S1 in SI). When the UV irradiation ceased, the shape was retained under room light. Subsequent visible light irradiation induced a reverse motion, i.e., the film gradually became flat and then curved upward as it was before UV irradiation (Figure 6A(c) and Movie S2 in SI). We observed similar bending−unbending behavior upon UV−vis irradiation on the reverse side of the film placed upside down (Figure 6B). We have repeated UV−vis irradiation on the same sample for more than seven cycles, and bending−unbending occurred each time without any detectable fatigue.

Thermal and mechanical properties of **H3** were further investigated. The thermogravimetry (TG) curves of **H3** (Figure S7 in SI) recorded in both air and N_2 atmosphere show almost no weight loss up to 200 °C. After heating in a 200 °C oven for 30 min, the lamellar structure of **H3** (Figure S8 in SI) was well retained without any structural deterioration, indicating its excellent thermal stability. The differential scanning calorimetry (DSC) curve of **H3** (Figure S9 in SI) showed no phase transition peaks in the temperature range 0−150 °C. This is different from the previously reported azobenzene-containing LC polymers which generally undergo phase transitions (glass state to elastomer state, smectic to nematic phase, or nematic to isotropic phase) and large deformations usually occur on photoinduced smectic-to-nematic or nematic-to-isotropic phase transitions above the glass transition temperature (T_g).[5]

The dynamic mechanical analysis of **H3** at room temperature shows that the storage modulus of **H3** (E' in Figure S10 in SI) is ca. 0.2 GPa, which is much superior to the rubbery LCEs (less than 1 MPa).[9a] The stress−strain curve obtained by tensile test (Figure S11 in SI) also confirmed the high elastic modulus of **H3** (0.23 GPa). The recently reported glassy LCNs have higher storage moduli (ca. 0.4−2.5 GPa,[8a−e,9,14b] 3.8−6.2 GPa[8f]). Their stiffness originates from the heavily cross-linked networks[8a−c,9] or high rigidity of polymer backbones.[8d−f] However, the increase in the modulus generally diminish the magnitude of bending,[8b,9a] though some improvements have been made by adjusting the azobenzene contents,[8e,9a] creating gradients in molecular alignments,[9] and by using high-intensity blue-green light irradiation.[14] Our hybrid film has achieved both relatively high stiffness and large amplitude of bending (bending angle of ca. 180°, as shown in Figure S12 in SI). This is ascribable to its hybrid composition and oriented lamellar structure. The flexible organic spacers and high content of ordered azobenzene moieties enable rapid, large amplitude of photoinduced bending. The 2D siloxane layer imparts mechanical strength in the in-plane direction, while keeping flexibility in the out-of-plane direction.

Bending−unbending behaviors of **H3** at elevated temperatures were investigated as shown in Figure 7. **H3** was put on a

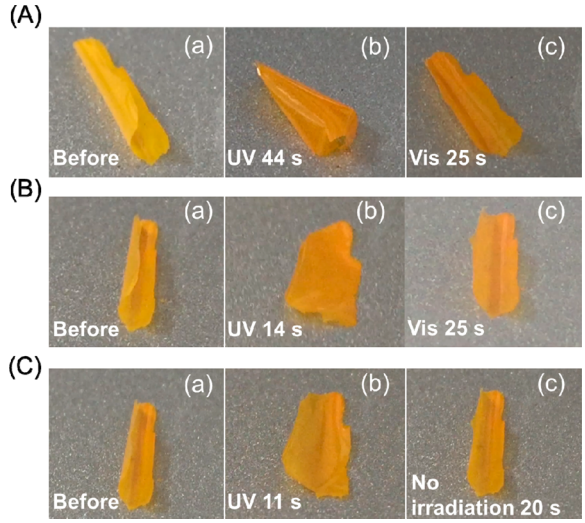

Figure 7. Photoinduced bending−unbending of **H3** on a hot plate at (A) 70 °C, (B) 100 °C, and (C) 130 °C. Film size: approximately 12 mm × 8 mm × 8 μm.

hot plate set at 70, 100, and 130 °C. The films at maximum bending and the corresponding irradiation times are shown (Figure 7(b)). At a relatively lower temperature (70 °C), UV-induced bending extent was larger. The film deformed from a concave shape to a convex shape within 44 s. The deformation process is fast as it became flat just after 7 s of UV irradiation (Movie S3 in SI). By further increasing the temperature, the maximum bending amplitude decreased. This can be explained by enhanced thermal *cis*-to-*trans* isomerization which resulted in a lower concentration of *cis* isomers in the photostationary state. Either visible light irradiation (Movie S4 in SI for film on the 70 °C hot plate) or just leaving the film on the hot plate (130 °C) after UV irradiation recovered the original shape rapidly (Figure 7(c)).

Photoinduced bending−unbending motions in azobenzene-containing LC polymer films have been reported to be caused

DOI: 10.1021/jacs.5b06172
J. Am. Chem. Soc. 2015, 137, 15434−15440

by expansion or contraction in the surface of the films.[5,13] The driving force is the reduction of structural order induced by *trans*−*cis* photoisomerization of azobenzene mesogens. Both mechanical strain in the surface and mechanical stress generated in the network should contribute to this out-of-plane deformation.[25b,29] In previous studies, photoinduced strain in glassy LCNs is smaller (ca. 0.5−2%) while that in LCEs is significantly larger (ca. 20% or larger);[8b] on the contrary, mechanical stress generated is large in the former and small in the latter. It is reported that the minor strain in the LC polymers is sufficient for bending.[5g] In our hybrid film, although no order reduction has been observed, photoinduced strain and mechanical stress are considered critical for bending. Due to the high concentration of azobenzene groups and the large thickness of **H3**, UV irradiation can induce *trans*-to-*cis* isomerization only in the surface region of the film (Figure 8(a)). Unlike LCEs where contraction or expansion is arising

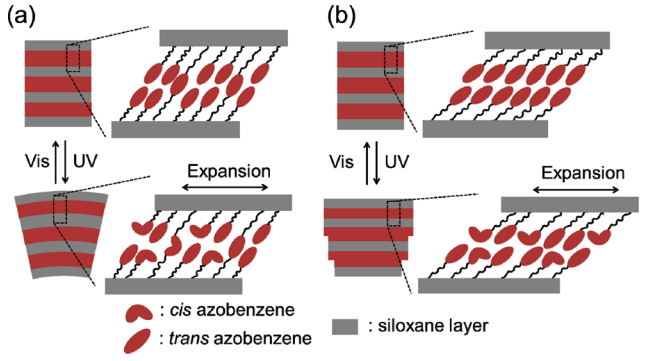

Figure 8. Schematic illustration of the different behaviors of (a) **H3** and (b) **H1** upon UV−vis irradiation. Only a limited number of layers are shown for simplification.

from the loss of the structural order, our hybrid material preserved the ordered structure after UV irradiation (Figure 4A). Because the bent *cis* isomers possess larger dimensions in the horizontal plane than the *trans* isomers, the decrease of the packing density should cause an expansion along the horizontal direction. Meanwhile mechanical stress was generated in the surface and transduced to the inner part of the film through the connected network, leading to bending of the film away from the UV source. Photoinduced bending of a silicone−azobenzene film was reported to occur by means of a compression (inner layer)−compression (outer layer) mode.[30] Considering the opposite direction of bending, it is reasonable to assume that the bending of **H3** occurs through a different mode involving an expansion of the layer exposed to the UV light,[5c] although the strain is too small to be measured at present. It can be calculated that 180° bending of the film with 7 mm length and 7 μm thickness (Figure S12 in SI) can be achieved by only a ca. 0.3% expansion difference between the top and bottom layers. A flexible, 2D siloxane layer is essential for such expansion of the film. The solid-state ^{29}Si CP/MAS NMR spectrum of **H3** (Figure 5b) showed signals at −48.0, −57.7, and −66.7 ppm, corresponding to the T^1, T^2, and T^3 (T^x: $CSi(OSi)_x(OH)_{3-x}$) silicon species, respectively. The presence of the T^1 and T^2 signals indicated that the siloxane network was not fully polycondensed, most likely due to the steric hindrance caused by two-dimensionally arranged organic moieties.[31] Such an incompletely polycondensed 2D network should allow for lateral expansion/contraction of the films upon UV−vis irradiation.

The partial cross-linking of siloxane layers by bridging azobenzene groups is critical for transducing mechanical stress. As mentioned above, the thick film (a small fragment) of **H1**, consisting solely of pendant azobenzene groups, did not show photoinduced bending. It is likely that the mechanical stress generated could not be transduced but relaxed[32] by sliding between the lamellae, as adjacent siloxane layers are not covalently connected (Figure 8(b)). The slight decrease in *d*-spacing (Figure 4) can be explained by lowering of the areal density of interlayer azobenzene groups upon expansion. If the degree of cross-linking is too high, such as in **H2**, the hybrid networks are too rigid to allow for expansion; therefore, neither *d*-spacing variation nor bending behavior were observed. Thus, proper bridging between the siloxane layers is important. Flexible, large area, free-standing films were also prepared with **P1**/**P2** ratios of 1:1, 2:1, 4:1, and 8:1; however, obvious photoinduced bending−unbending motions were observed only when the ratio was 4:1.

Compared to the azobenzene-containing LC polymer films capable of bending−unbending motions, the present system has several features. The facile formation of an oriented lamellar structure by simple sol−gel processing through self-assembly is fundamentally different from the LC polymer fabrication, which relies on the use of a rubbed polyimide coating as an alignment layer[5] or hot pressing processes[7] to form oriented structures.

The attracting features of our hybrid film are its good mechanical strength and thermal stability, accompanied by the photoinduced reversible bending−unbending over a wide range of temperature. It shows fast, large amplitude of bending similar to that reported for LCEs,[5] while possessing relatively high storage modulus comparable to some of the glassy LCNs.[8a] It should be noted that high-modulus glassy LCNs generally require extremely high intensity of UV irradiation (ca. 1.0 W/cm^2)[14] to overcome the low magnitude of bending.[8e,f] The UV intensity we employed here is modest, less than 1.5 mW/cm^2. Rather large amplitude of deformation induced by such relatively weak UV irradiation is of practical importance. In addition, heat often exerts great influence on the bending instead of light in glassy LCNs.[9c,12] Photoactuation from room temperature up to 130 °C observed for our material is desirable for use under scorching conditions. The photoinduced bending−unbending was also observed in an aqueous environment (Figure S13 in SI), which allows application in microfluidics.[12]

■ CONCLUSIONS

We have demonstrated a new class of photoresponsive azobenzene−siloxane hybrid materials prepared by a simple self-assembly process using organoalkoxysilane precursors containing pendant and bridging azobenzene groups via flexible spacers. The hybrid film from the pendant-type precursor exhibited large, quick, reversible photoinduced *d*-spacing variation upon light irradiation. Through cohydrolysis and polycondensation of these two precursors, a free-standing film displaying a large magnitude of bending−unbending motion over a wide temperature range upon UV−vis irradiation has been successfully prepared. The film possesses relatively high storage modulus and good thermal stability arising from its unique lamellar structure consisting of azobenzene layers and 2D siloxane layers, which is quite different from the structures of conventional LC polymers. Partial cross-linking of the

DOI: 10.1021/jacs.5b06172
J. Am. Chem. Soc. 2015, 137, 15434−15440

adjacent siloxane layers with bridging azobenzene groups was also the key to realize photoinduced bending motions. Fine tuning of the structures and properties will be achieved by further molecular design of the precursors. This novel hybrid system will open new research fields as well as vast applications for smart devices and energy conversion devices.

EXPERIMENTAL SECTION

Materials. Poly(vinyl alcohol) (PVA, MW = 22 000), toluene (super dehydrated, > 99.5%), and tetrahydrofuran (THF, no stabilizer, > 99.5%) were purchased from Wako Pure Chemical Industries, Ltd. 3-Mercaptopropyltriethoxysilane (MPTES, > 95.0%) and azobis(isobutyronitrile) (AIBN, > 98.0%) were purchased from Tokyo Chemical Industry Co., Ltd. All chemicals were used as received.

Synthesis of a Triethoxysilyl Precursor with a Pendant Azobenzene Group (P1). 4-Allyloxy-azobenzene was synthesized as previously reported.[27] The thiol−ene reaction of 4-allyloxy-azobenzene (0.476 g, 0.002 mol) with an excess amount of MPTES (0.952 g, 0.004 mol) was performed in toluene (8 mL) in the presence of AIBN as an initiator (0.016 g, 0.0001 mol). After stirring the mixture at 80 °C for 10 h under a nitrogen atmosphere, the solvent and unreacted MPTES were removed in vacuo. **P1** was obtained as an orange liquid (0.392 g, 41% yield) after purification using gel permeation chromatography (GPC) with chloroform as the eluent. ^{1}H NMR (δ, 500 MHz, $CDCl_3$): 0.72−0.75 (t, 2H, $SCH_2CH_2CH_2Si$), 1.20−1.23 (t, 9H, $SiOCH_2CH_3$), 1.69−1.75 (m, 2H, $SCH_2CH_2CH_2Si$, 2.02−2.08 (m, 2H, $ArOCH_2CH_2CH_2S$), 2.53−2.56 (t, 2H, $SCH_2CH_2CH_2Si$, 2.66−2.69 (t, 2H, $ArOCH_2CH_2CH_2S$), 3.79−3.83 (m, 6H, $SiOCH_2CH_3$), 4.07−4.10 (t, 2H, $ArOCH_2CH_2CH_2S$), 6.96−6.98 (d, 2H, ArH), 7.37−7.40 (t, 1H, ArH), 7.44−7.47 (t, 2H, ArH), 7.86−7.91 (m, 4H, ArH). ^{13}C NMR (δ, 125.7 MHz, $CDCl_3$): 9.92, 18.34, 23.25, 28.31, 29.29, 35.19, 58.35, 66.58, 114.73, 122.61, 124.79, 128.98, 130.30, 147.02, 152.80, 161.45. ^{29}Si NMR (δ, 99.3 MHz, $CDCl_3$): −45.83. ESI-MS: m/z 499.2 $[M + Na]^+$.

Synthesis of a Bis-triethoxysilyl Precursor with a Bridging Azobenzene Group (P2). 4,4′-Diallyloxy-azobenzene was synthesized as previously reported.[27] **P2** was synthesized by the thiol−ene reaction of 4,4′-diallyloxy-azobenzene (0.290 g, 0.001 mol) with an excess amount of MPTES (1.430 g, 0.006 mol) in toluene (8 mL) in the presence of AIBN (0.016 g, 0.0001 mol). The mixture was stirred at 80 °C for 10 h under a nitrogen atmosphere, after which the solvent and unreacted MPTES were removed in vacuo. **P2** was obtained as an orange liquid (0.427 g, 55% yield) after purification using GPC with chloroform as the eluent. ^{1}H NMR (δ, 500 MHz, $CDCl_3$): 0.73−0.76 (t, 4H, $SCH_2CH_2CH_2Si$), 1.21−1.24 (t, 18H, $SiOCH_2CH_3$), 1.69−1.76 (m, 4H, $SCH_2CH_2CH_2Si$), 2.05−2.10 (m, 4H, $ArOCH_2CH_2CH_2S$), 2.55−2.58 (t, 4H, $SCH_2CH_2CH_2Si$, 2.68−2.73 (4H, $ArOCH_2CH_2CH_2S$), 3.80−3.84 (m, 12H, $SiOCH_2CH_3$), 4.11−4.15 (t, 4H, $ArOCH_2CH_2CH_2S$), 6.97−6.99 (d, 4H, ArH), 7.85−7.87 (d, 4H, ArH). ^{13}C NMR (δ, 125.7 MHz, $CDCl_3$): 9.89, 18.32, 23.21, 28.34, 29.30, 35.18, 58.37, 66.59, 114.67, 124.33, 147.11, 160.78. ^{29}Si NMR (δ, 99.3 MHz, $CDCl_3$): −45.76. ESI-MS: m/z 793.3 $[M + Na]^+$.

Preparation of Supported Hybrid Thin Films (H1 and H2) via Hydrolysis and Polycondensation of P1 and P2. An aqueous solution of HCl was added to THF solutions of **P1** and **P2**. The mixtures with molar ratios of **P1**:THF:H_2O:HCl = 1:65:20:0.04 and **P2**:THF:H_2O:HCl = 1:50:15:0.03 were stirred at room temperature for 4 h and 30 min, respectively. Note that these conditions were adjusted to obtain ordered structures. Smaller amounts of H_2O and HCl and shorter hydrolysis time were applied to **P2** because of its higher cross-linking ability. A portion of each solution was spin-coated on a glass substrate to obtain the thin films. Supported hybrid films (**H1** and **H2**) were obtained after heating at 80 °C for 5 h to induce polycondensation.

Preparation of Free-Standing Film (H3) via Cohydrolysis and Polycondensation of P1 and P2. H3 was prepared by cohydrolysis and polycondensation of **P1** and **P2**. The molar ratio of the starting mixture was **P1**:**P2**:THF:H_2O:HCl = 1:0.25:65:20:0.04. After being stirred for 4 h, the mixture was cast on a PVA-coated glass substrate (prepared by spin-coating of a 10 wt % aqueous solution of PVA). We confirmed that the PVA film did not dissolve in a THF/H_2O solution (molar ratio of 65:20). After heating in air at 80 °C for 5 h, the cast film on the substrate was immersed in water for several days to detach the film from the substrate. The resulting free-standing film was dried at 60 °C for several hours before photoirradiation examination.

Characterization. Liquid-state ^{1}H, ^{13}C, and ^{29}Si nuclear magnetic resonance (NMR) spectra were recorded on a Bruker AVANCE 500 spectrometer with resonance frequencies of 500.0, 125.7, and 99.3 MHz, respectively, using $CDCl_3$ as the solvent and tetramethylsilane as the internal standard. The solid-state ^{29}Si cross-polarization magic-angle spinning (CP/MAS) NMR spectrum was recorded on a JEOL JNM-ECX-400 spectrometer at a resonance frequency of 79.4 MHz with a contact time of 5 ms and a recycle delay of 8 s. High-resolution electrospray ionization mass spectrometry (ESI-MS) analysis of the precursors dissolved in methanol was carried out with JEOL JMS-T100CS. X-ray diffraction (XRD) patterns with Bragg−Brentano geometry were obtained using a Rigaku Ultima IV diffractometer operated at 40 kV and 40 mA with Cu Kα radiation. The measurements were performed at a scanning speed of 1° min^{-1} with a step width of 0.02°. 2D-XRD patterns were recorded in reflection mode with Rigaku NANO-Viewer equipped with a Pilatus 2D X-ray detector (Dektris) using Cu Kα radiation (40 kV and 30 mA). The incident angle was 0.2° and the sample−detector distance was 730 mm. FT-IR spectra were recorded on a JASCO FT/IR-6100 spectrometer by the KBr pellet technique. The transmission electron microscopy (TEM) image was recorded on a JEOL JEM-2010 electron microscope at an accelerating voltage of 200 kV. UV−vis absorption spectra were recorded on JASCO V-670. Thermogravimetry (TG) measurements were conducted on a Rigaku Thermo Plus 2 instrument in air or nitrogen atmosphere with a heating rate of 5 °C per min. Differential scanning calorimetry (DSC) measurement was performed on Shimadzu DSC60plus with a heating rate of 10 °C per min in nitrogen atmosphere. Dynamic mechanical analysis was conducted using a nonresonance forced vibration viscoelastometer (Rheogel-E-4000F; UBM, Kyoto, Japan) in the tension mode. The frequency and amplitude of the vibration were adjusted to 80 Hz and 2 μm, respectively. The sample dimension was approximately 4 mm × 20 mm × 10 μm. UV and visible light irradiation were performed with a 200 W Hg/Xe lamp (San-ei electric UVF-204S) equipped with UV pass (HOYA U-340) and UV cut (HOYA L42) filters, respectively.

ASSOCIATED CONTENT

Supporting Information

The Supporting Information is available free of charge on the ACS Publications website at DOI: 10.1021/jacs.5b06172.

Figures S1−S13. (PDF)
Movie S1. (MPG)
Movie S2. (MPG)
Movie S3. (MPG)
Movie S4. (MPG)

AUTHOR INFORMATION

Corresponding Author

*shimojima@waseda.jp

Notes

The authors declare no competing financial interest.

ACKNOWLEDGMENTS

We thank Mr. Yuta Shimasaki (Waseda University) for TEM observation, Mr. Hidehiro Tsuzura (Waseda University) for ^{29}Si CP/MAS NMR measurement, Mr. Shintaro Hara (Waseda University) for 2D-XRD measurements, Mr. Daiki Tomori (Doshisha University), who is researching at OMTRI, for DSC measurement, and Mr. Takafumi Noguchi (Kansai University)

DOI: 10.1021/jacs.5b06172
J. Am. Chem. Soc. 2015, 137, 15434−15440

for dynamic mechanical analysis and tensile test. This work was supported in part by a Grant-in-Aid for Scientific Research on Innovative Areas "New Polymeric Materials Based on Element-Blocks (No. 2401)" provided by The Ministry of Education, Culture, Sports, Science and Technology, Japan.

REFERENCES

(1) (a) Ercole, F.; Davis, T. P.; Evans, R. A. *Polym. Chem.* **2010**, *1*, 37. (b) Yagai, S.; Kitamura, A. *Chem. Soc. Rev.* **2008**, *37*, 1520. (c) Seki, T. *Macromol. Rapid Commun.* **2014**, *35*, 271. (d) Priimagi, A.; Barrett, C. J.; Shishido, A. *J. Mater. Chem. C* **2014**, *2*, 7155.

(2) (a) Anzai, J.; Osa, T. *Tetrahedron* **1994**, *50*, 4039. (b) Bandara, H. M. D.; Burdette, S. C. *Chem. Soc. Rev.* **2012**, *41*, 1809.

(3) Finkelmann, H.; Nishikawa, E.; Pereira, G. G.; Warner, M. *Phys. Rev. Lett.* **2001**, *87*, 015501−1.

(4) Li, M.-H.; Kellar, P.; Li, B.; Wang, X.; Brunet, M. *Adv. Mater.* **2003**, *15*, 569.

(5) (a) Yu, Y.; Nakano, M.; Ikeda, T. *Nature* **2003**, *425*, 145. (b) Ikeda, T.; Nakano, M.; Yu, Y.; Tsutsumi, O.; Kanazawa, A. *Adv. Mater.* **2003**, *15*, 201. (c) Kondo, M.; Yu, Y.; Ikeda, T. *Angew. Chem., Int. Ed.* **2006**, *45*, 1378. (d) Lv, J.; Wang, W.; Xu, J.; Ikeda, T.; Yu, Y. *Macromol. Rapid Commun.* **2014**, *35*, 1266. (e) Zhang, Y.; Xu, Y.; Cheng, F.; Yin, R.; Yen, C.-C.; Yu, Y. *J. Mater. Chem.* **2010**, *20*, 7123. (f) Naka, Y.; Mamiya, J.; Shishido, A.; Washio, M.; Ikeda, T. *J. Mater. Chem.* **2011**, *21*, 1681. (g) Shimamura, A.; Priimagi, A.; Mamiya, J.; Kinoshita, M.; Ikeda, T.; Shishido, A. *J. Nonlinear Opt. Phys. Mater.* **2011**, *20*, 405.

(6) Cervera-Procas, R.; Sánchez-Somolinos, C.; Serrano, J. L.; Omenat, A. *Macromol. Rapid Commun.* **2013**, *34*, 498.

(7) Hosono, N.; Kajitani, T.; Fukushima, T.; Ito, K.; Sasaki, S.; Takata, M.; Aida, T. *Science* **2010**, *330*, 808.

(8) (a) Wie, J. J.; Lee, K. M.; Smith, M. L.; Vaia, R. A.; White, T. J. *Soft Matter* **2013**, *9*, 9303. (b) Lee, K. M.; Tabiryan, N. V.; Bunning, T. J.; White, T. J. *J. Mater. Chem.* **2012**, *22*, 691. (c) Lee, K. M.; Koerner, H.; Vaia, R. A.; Bunnning, T. J.; White, T. J. *Soft Matter* **2011**, *7*, 4318. (d) Wang, D. H.; Wie, J. J.; Lee, K. M.; White, T. J.; Tan, L.-S. *Macromolecules* **2014**, *47*, 659. (e) Wang, D. H.; Lee, K. M.; Yu, Z.; Koerner, H.; Vaia, R. A.; White, T. J.; Tan, L.-S. *Macromolecules* **2011**, *44*, 3840. (f) Lee, K. M.; Wang, D. H.; Koerner, H.; Vaia, R. A.; Tan, L.-S.; White, T. J. *Angew. Chem.* **2012**, *124*, 4193.

(9) (a) Harris, K. D.; Cuypers, R.; Scheibe, P.; van Oosten, C. L.; Bastiaansen, C. W. M.; Lub, J.; Broer, D. J. *J. Mater. Chem.* **2005**, *15*, 5043. (b) van Oosten, C. L.; Corbett, D.; Davies, D.; Warner, M.; Bastiaansen, C. W. M.; Broer, D. J. *Macromolecules* **2008**, *41*, 8592. (c) van Oosten, C. L.; Harris, K. D.; Bastiaansen, C. W. M.; Broer, D. J. *Eur. Phys. J. E: Soft Matter Biol. Phys.* **2007**, *23*, 329.

(10) Yamada, M.; Kondo, M.; Mamiya, J.; Yu, Y.; Kinoshita, M.; Barrett, C. J.; Ikeda, T. *Angew. Chem., Int. Ed.* **2008**, *47*, 4986.

(11) Yamada, M.; Kondo, M.; Miyasato, R.; Naka, Y.; Mamiya, J.; Kinoshita, M.; Shishido, A.; Yu, Y.; Barrett, C. J.; Ikeda, T. *J. Mater. Chem.* **2009**, *19*, 60.

(12) van Oosten, C. L.; Bastiaansen, C. W. M.; Broer, D. J. *Nat. Mater.* **2009**, *8*, 677.

(13) Ikeda, T.; Ube, T. *Mater. Today* **2011**, *14*, 480.

(14) (a) White, T. J.; Tabiryan, N. V.; Serak, S. V.; Hrozhyk, U. A.; Tondiglia, V. P.; Koerner, H.; Vaia, R. A.; Bunning, T. J. *Soft Matter* **2008**, *4*, 1796. (b) Lee, K. M.; Smith, M. L.; Koerner, H.; Tabiryan, N.; Vaia, R. A.; Bunning, T. J.; White, T. J. *Adv. Funct. Mater.* **2011**, *21*, 2913.

(15) (a) Ogawa, M.; Ishii, T.; Miyamoto, N.; Kuroda, K. *Appl. Clay Sci.* **2003**, *22*, 179. (b) Ogawa, M.; Ishii, T.; Miyamoto, N.; Kuroda, K. *Adv. Mater.* **2001**, *13*, 1107.

(16) (a) Nabetani, Y.; Takamura, H.; Hayasaka, Y.; Shimada, T.; Takagi, S.; Tachibana, H.; Masui, D.; Tong, Z.; Inoue, H. *J. Am. Chem. Soc.* **2011**, *133*, 17130. (b) Nabetani, Y.; Takamura, H.; Hayasaka, Y.; Sasamoto, S.; Tanamura, Y.; Shimada, T.; Masui, D.; Takagi, S.; Tachibana, H.; Tong, Z.; Inoue, H. *Nanoscale* **2013**, *5*, 3182.

(17) Abellán, G.; Coronado, E.; Martí-Gastaldo, C.; Ribera, A.; Jordá, J. L.; García, H. *Adv. Mater.* **2014**, *26*, 4156.

(18) (a) Liu, N.; Dunphy, D. R.; Rodriguez, M. A.; Singer, S.; Brinker, J. *Chem. Commun.* **2003**, 1144. (b) Liu, N.; Chen, Z.; Dunphy, D. R.; Jiang, Y.-B.; Assink, R. A.; Brinker, C. J. *Angew. Chem., Int. Ed.* **2003**, *42*, 1731. (c) Liu, N.; Dunphy, D. R.; Atanassov, P.; Bunge, S. D.; Chen, Z.; López, G. P.; Boyle, T. J.; Brinker, C. J. *Nano Lett.* **2004**, *4*, 551. (d) Zhu, Y.; Fujiwara, M. *Angew. Chem., Int. Ed.* **2007**, *46*, 2241.

(19) Tanaka, T.; Ogino, H.; Iwamoto, M. *Langmuir* **2007**, *23*, 11417.

(20) (a) Angelos, S.; Yang, Y.-W.; Khashab, N. M.; Stoddart, J. F.; Zink, J. I. *J. Am. Chem. Soc.* **2009**, *131*, 11344. (b) Angelos, S.; Choi, E.; Vögtle, F.; Cola, L. D.; Zink, J. I. *J. Phys. Chem. C* **2007**, *111*, 6589. (c) Lu, J.; Choi, E.; Tamanoi, F.; Zink, J. I. *Small* **2008**, *4*, 421.

(21) Mitran, R.-A.; Berger, D.; Băjenaru, L.; Năstase, S.; Andronescu, C.; Matei, C. *Cent. Eur. J. Chem.* **2014**, *12*, 788.

(22) Alvaro, M.; Benitez, M.; Das, D.; Garcia, H.; Peris, E. *Chem. Mater.* **2005**, *17*, 4958.

(23) Besson, E.; Mehdi, A.; Lerner, D. A.; Reyé, C.; Corriu, R. J. P. *J. Mater. Chem.* **2005**, *15*, 803.

(24) (a) Shimojima, A.; Kuroda, K. *Chem. Rec.* **2006**, *6*, 53. (b) Chemtob, A.; Ni, L.; Croutxé-Barghorn, C.; Boury, B. *Chem. - Eur. J.* **2014**, *20*, 1790.

(25) (a) Camacho-Lopez, M.; Finkelmann, H.; Palffy-Muhoray, P.; Shelley, M. *Nat. Mater.* **2004**, *3*, 307. (b) Sánchez-Ferrer, A.; Finkelmann, H. *Soft Matter* **2013**, *9*, 4621.

(26) Liu, N.; Yu, K.; Smarsly, B.; Dunphy, D. R.; Jiang, Y.-B.; Brinker, C. J. *J. Am. Chem. Soc.* **2002**, *124*, 14540.

(27) (a) Guo, S.; Sugawara-Narutaki, A.; Okubo, T.; Shimojima, A. *J. Mater. Chem. C* **2013**, *1*, 6989. (b) Guo, S.; Chaikittisilp, W.; Okubo, T.; Shimojima, A. *RSC Adv.* **2014**, *4*, 25319.

(28) Deng, Y.; Li, Y.; Wang, X. *Macromolecules* **2006**, *39*, 6590.

(29) Kondo, M.; Sugimoto, M.; Yamada, M.; Naka, Y.; Mamiya, J.; Kinoshita, M.; Shishido, A.; Yu, Y.; Ikeda, T. *J. Mater. Chem.* **2010**, *20*, 117.

(30) Akamatsu, N.; Tashiro, W.; Saito, K.; Mamiya, J.; Kinoshita, M.; Ikeda, T.; Takeya, J.; Fujikawa, S.; Priimagi, A.; Shishido, A. *Sci. Rep.* **2014**, *4*, 5377.

(31) Shimojima, A.; Sugahara, Y.; Kuroda, K. *Bull. Chem. Soc. Jpn.* **1997**, *70*, 2847.

(32) Priimagi, A.; Shimamura, A.; Kondo, M.; Hiraoka, T.; Kubo, S.; Mamiya, J.; Kinoshita, M.; Ikeda, T.; Shishido, A. *ACS Macro Lett.* **2012**, *1*, 96.

DOI: 10.1021/jacs.5b06172
J. Am. Chem. Soc. 2015, 137, 15434−15440